ELSEVIER

CrossMark

Urologic Oncology: Seminars and Original Investigations 35 (2017) 300–309

UROLOGIC ONCOLOGY

Original article

Filtration-based enrichment of circulating tumor cells from all prostate cancer risk groups

Julius Adebayo Awe, M.B.B.S.[a,b,c], Jeff Saranchuk, M.D.[d], Darrel Drachenberg, M.D.[d], Sabine Mai, Ph.D.[a,*]

[a] *Manitoba Institute of Cell Biology, University of Manitoba, CancerCare Manitoba, 675 McDermot Ave, Winnipeg, Manitoba, Canada MB R3E 0V9*
[b] *Systems Biology Research Centre, School of Life Sciences, University of Skövde, Skövde, Sweden*
[c] *Department of Clinical Genetics, Institute of Biomedicine, Sahlgrenska Academy, University of Gothenburg, Gothenburg, Sweden*
[d] *Department of Surgery, Manitoba Prostate Center, University of Manitoba, Winnipeg, Manitoba, Canada*

Received 15 July 2016; received in revised form 14 December 2016; accepted 15 December 2016

Abstract

Objective: To combine circulating tumor cell (CTC) isolation by filtration and immunohistochemistry to investigate the presence of CTCs in low, intermediate, and high-risk prostate cancer (PCa). CTCs isolated from these risk groups stained positive for both cytokeratin and androgen receptors, but negative for CD45.

Patients and methods: Blood samples from 41 biopsy confirmed patients with PCa at different clinical stages such as low, intermediate, and high risk were analyzed. The samples were processed with the ScreenCell filtration device and PCa CTCs were captured for all patients. The isolated CTCs were confirmed PCa CTCs by the presence of androgen receptors and cytokeratins 8, 18, and 19 that occurred in the absence of CD45 positivity. PCa CTC nuclear sizes were measured using the TeloView program.

Results: The filtration-based isolation method used permitted the measurement of the average nuclear size of the captured CTCs. CTCs were identified by immunohistochemistry in low, intermediate, and high-risk groups of patients with PCa.

Conclusion: CTCs may be found in all stages of PCa. These CTCs can be used to determine the level of genomic instability at any stage of PCa; this will, in the future, enable personalized patient management.

Keywords: Prostate cancer; Circulating tumor cells; Androgen receptors; Cytokeratin; Filter isolation

1. Introduction

The description of tumor cells in the blood circulation by Thomas Ashworth [1], ushered a promising field in cancer research where neoplastic cells are isolated then characterized for prognostic and therapeutic design purposes. However, the field of circulating tumor cell (CTC) research has been challenged by the rarity of CTCs in circulation (numbers as low as 1 CTC in every 1 million blood cells have been proposed) [2], the presence of multiple CTC subpopulations in the same patients with cancer [3], the short life span of CTCs in bloodstream and adaptations of CTCs to circulation [4], which leads to loss of unique attributes observed in the parent tumor [3,5,6].

Despite these challenges, many techniques have evolved for the isolation of CTCs based on their physical and immunological properties, with varying results. The size-based filtration technique was chosen for this study owing to its ability to isolate CTCs without the need for antibody detection [3,4,7–9]. The filtration technique preserves the CTC morphology and maintains the presence of CTC clusters. The ScreenCell filters [4], used in this study, are adapted for key biochemical analysis such as FISH, immunohistochemistry, cell culture, PCR, and three-dimensional (3D) imaging [3].

Prostate cancer (PCa) is the most common solid neoplasm in men in western countries with a high incidence rate of 24% of all new cancer cases and 10% of all cancer deaths in

* Corresponding author. Tel.: +1-204-787-2135; fax: +1-204-787-2190.
E-mail address: Sabine.Mai@umanitoba.ca (S. Mai).

http://dx.doi.org/10.1016/j.urolonc.2016.12.008

Canada according to the Canadian Cancer Society [10]. Inaccurate clinical staging of PCa leads to avoidable surgical intervention with associated complications in some patients. Data from CTC research present an opportunity to potentially improve diagnosis, prognosis, and the overall management of PCa. This study documents an effective PCa CTC isolation technique coupled with staining for androgen receptor (AR); cytokeratin 8, 18, and 19; CD45 negativity; and nuclear DNA with 4', 6-diamindino-2 phenylindole (DAPI) to enable subsequent analyses of verified PCa CTCs.

2. Materials and methods

2.1. Patients

Overall, 41 patients with biopsy confirmed PCa were included in this study. Further, 5 low-risk patients, 34 intermediate-risk patients, 3 high risk, and 3 female control blood samples from patients with no medical history of cancer (Table). The patients were risk classified according to the D'Amico classification for survival, which makes use of the clinical staging (TNM), Gleason score of biopsy, prostate specific antigen, and age of the patient [11]. The Research Ethics Board on human studies at University of Manitoba approved the study with ethics reference number HS14085 (H2011: 336). Blood samples analyzed were obtained from patients before surgery. During analysis of the samples, clinical data were blinded to eliminate potential bias.

2.2. Filter device

ScreenCell filtration, a size-based enrichment technique with European CE mark and Health Canada approval (License no. 7044), was used to isolate PCa CTCs from the blood of patients with PCa. It consists of a filter membrane attached to a metal ring placed between a filtration reservoir and a removable nozzle holder (ScreenCell). The filter membrane contains pores with diameter of 7.5 ± 0.36 µm that are randomly distributed throughout the membrane (1×10^5 pores/cm^2). Overall, 4 ml of ScreenCell buffer (ScreenCell) are incubated at room temperature with 3 ml of blood for 8 minutes. The ScreenCell buffer added to the blood sample lyses the red blood cells, prefixes all nucleated cells present in the sample while preserving their architecture and enabling their fixation onto the filter membrane of the device. Thereafter, this mix is passed through the microporous membrane filter, the process of filtration takes less than 5 minutes. Desitter et al. [4] validated this technique by filtration of CTC-spiked cells and this resulted in an average CTC recovery rate of 91.2%. Biochemical processing of the CTCs such as immunohistochemistry, DNA staining, or FISH can be subsequently done on the filters.

3. Immunohistochemistry with cytokeratin and androgen receptor antibodies

3.1. Cytokeratin staining of CTCs

CTCs on the filter are fixed with 3.7% formaldehyde/1× phosphate buffered saline (PBS) for 10 minutes, washed 3 times 3 minutes each with 50 mM $MgCl_2$/1xPBS, and blocked with 50 µl of fetal bovine serum for 30 minutes. The filters are then incubated for 45 minutes at 37°C in a humidified chamber after adding 50 µl of 5 µg/ml cytokeratin 8, 18, and 19 (Abcam Inc., Toronto, Ontario, Canada). The filters are washed, blocked, and 50 µl of Goat antimouse IgG-Alexa 488 (1 µg/ml) (Life Technologies Inc., Burlington, ON, Cat #A11029, Lot/Batch 44094A) are added to incubate for 45 minutes. The filter placed onto microscope slides, covered with cover slips after a coat with Vectashield (Vector Laboratories, Burlington, Ontario, Canada) reagent to minimize photo bleaching.

3.2. Combined androgen receptor and CD45 staining of CTCs

Captured cells on the ScreenCell filters are incubated at room temperature with 3.7% formaldehyde/1× phosphate buffered saline (PBS) for 10 minutes, washed 3 times 3 minutes each with 50 mM $MgCl_2$. Permeabilized with 0.1% Triton X-100 (in ddH_2O) for 12 minutes no shaking, washed 3 times 3 minutes each with 50 mM $MgCl_2$/1xPBS. The filters were incubated for 45 minutes at 37°C in a humidified chamber after 25 µl of AR antibody (441): sc-7305 (Santa Cruz Biotechnologies Inc., Dallas, TX) conjugated with Alexa Fluor 488 at 4 µg/ml and 25 µl of rat antihuman CD45 (Clone YAML501.4; Ref: MA5-17687; Thermo Fisher: 3747 N. Meridian Road Rockford, IL 61105 USA) were applied to the cells on the filter. The filters with the cells go through 3 washes 3 minutes each, and are then mounted on slides. Vectashield (Vector Laboratories, Burlington, ON, Canada) with DAPI was applied on them to stain the nuclear DNA.

4. Three-dimensional image acquisition

Images are acquired using a Zeiss AxioImager Z2 microscope (Carl Zeiss Ltd., Toronto, ON), equipped with AxioCam HR B&W camera and 63×/1.4 oil objective. Thirty 3D interphase nuclei of captured PCa CTCs were imaged and deconvolved for analysis (Fig. 1A). Deconvolution of the images was performed with a constrained iterative algorithm [12]. The reconstructed 3D images were then exported as tif files into TeloView (3D Signatures Inc., Winnipeg, MB, Canada) program for analysis [12].

Table
Clinical and CTC information of patients examined. This shows the PSA, management, Gleason score, risk class, average nuclear volume and average nuclear diameter of the 41 patients in this study. It is noted that that the absolute PSA values and the average nuclear diameter does not correspond with the risk classes of the patients

Patient ID	PSA, μg/l (MM/YY)	Management (MM/YY)	Gleason score by TRUS	Clinical risk stratification	Average nuclear diameter (μm)	Average nuclear volume (μm^3)
MB221-06-12	5.13 (05/12)	Dutasteride (11/10)	3 + 3	Low risk	11.1	721.4
MB221-12-12	7.39 (11/12)		3 + 3	Low risk	9.1	392
MB239-08-12	5.4 (07/12)	No treatment	3 + 3	Low risk	10.8	655.9
MB239-05-13	6.11 (04/13)		3 + 3	Low risk	11.81	862.5
MB244-08-12	3.1 (08/12)	Dutasteride (08/12)	3 + 3	Low risk	15.4	1916.9
MB244-05-14	1.40 (04/14)		3 + 3	Low risk	11.5	789.9
MB268-11-12	9.47 (11/12)	No treatment	3 + 3	Low risk	15.1	1816.5
MB268-06-13	9.50 (08/13)	No treatment	3 + 3	Low risk	10.1	540.1
MB276-12-12	9.05 (10/12)	RP (01/13)	3 + 3	Low risk	10.6	629.8
MB276-05-13	0.03 (04/13)		3 + 3	Low risk	11.9	893.9
MB138-06-12	0.01 (06/12)	RP (06/11)	3 + 4	Favorable intermediate risk	10.6	617.7
MB138-12-12	0.01 (12/12)		3 + 4	Favorable intermediate risk	12.4	989.5
MB199-04-13	0.09 (03/13)	RP/(06/12)	3 + 4	Favorable intermediate risk	11.7	846.5
MB199-09-13	0.01 (09/13)		3 + 4	Favorable intermediate risk	13.4	1246.6
MB228-07-12	0.01 (06/12)	RP/(03/09)	3 + 4	Favorable intermediate risk	13.9	1430.1
MB228-08-13	0.01 (08/12)		3 + 4	Favorable intermediate risk	10.7	637.3
MB245-08-12	8.26 (06/12)	No treatment	3 + 4	Favorable intermediate risk	12.8	1104.3
MB234-08-12	4.08 (05/12)	No treatment	3 + 4	Favorable intermediate risk	12.8	1110.5
MB235-08-12	5.71 (11/12)	No treatment	3 + 4	Favorable intermediate risk	11.3	747.1
MB267-11-12	14.57 (08/12)	No treatment	3 + 4	Favorable intermediate risk	15.1	1811.6
MB269-11-12	2.32 (11/12)	No treatment	3 + 4	Favorable intermediate risk	10.8	652.7
MB316-04-13	4.95 (04/13)	No treatment	3 + 4	Favorable intermediate risk	11.7	834.8
MB330-05-13	5.36 (10/12)	No treatment	3 + 4	Favorable intermediate risk	10.9	676.0
MB339-07-13	11.33 (02/13)	No treatment	3 + 4	Favorable intermediate risk	12.8	1101.6
MB353-09-13	3.84 (09/13)	No treatment	3 + 4	Favorable intermediate risk	12.8	1090.2
MB376-11-13	19.73 (07/13)	No treatment	3 + 4	Favorable intermediate risk	11.1	718.2
MB390-01-14	1.23 (08/13)	No treatment	3 + 4	Favorable intermediate risk	11.4	780.5
MB399-01-14	3.26 (09/13)	No treatment	3 + 4	Favorable intermediate risk	11.9	880.0
MB414-04-14	15.78 (02/14)	No treatment	3 + 4	Favorable intermediate risk	13.9	1413.4
MB434-04-14	10.30 (12/13)	No treatment	3 + 4	Favorable intermediate risk	22.6	6043.4
MB462-08-14	11.83 (05/14)	No treatment	3 + 4	Favorable intermediate risk	12.5	1015.3
MB465-08-14	5.76 (02/14)	No treatment	3 + 4	Favorable intermediate risk	14.5	1581.6
MB472-09-14	9.5 (09/14)	No treatment	3 + 4	Favorable intermediate risk	15.4	1895.6
MB473-09-14	8.3 (09/14)	No treatment	3 + 4	Favorable intermediate risk	16.1	2187.4
MB243-08-12	7.6 (09/12)	No treatment	4 + 3	Unfavorable intermediate risk	11.81	490.1
MB251-05-13	3.03 (05/13)	Finasteride (07/10)	4 + 3	Unfavorable intermediate risk	10.6	621.2
MB251-09-13	3.03 (05/13)	Finasteride (07/10)	4 + 3	Unfavorable intermediate risk	9.4	435.1
MB258-10-12	8.07 (05/12)	No treatment	4 + 3	Unfavorable intermediate risk	11.1	717.1
MB264-11-12	22.43 (11/12)	No treatment	4 + 3	Unfavorable intermediate risk	12.9	1125.9
MB272-12-12	14.71 (10/12)	No treatment	4 + 3	Unfavorable intermediate risk	10.4	591
MB304-03-13	16.7 (03/13)	No treatment	4 + 3	Unfavorable intermediate risk	12.3	979.6
MB312-04-13	6.55 (04/13)	No treatment	4 + 3	Unfavorable Intermediate Risk	12.8	1093.3
MB377-11-13	5.02 (08/13)	No treatment	4 + 3	Unfavorable intermediate risk	11.8	868.2
MB403-01-14	8.92 (12/13)	No treatment	4 + 3	Unfavorable intermediate risk	9.8	489.2
MB416-03-14	0.01 (03/14)	No treatment	4 + 3	Unfavorable intermediate risk	15.6	1969.6
MB417-03-14	9.66 (03/14)	No treatment	4 + 3	Unfavorable intermediate risk	15.6	1982.5
MB467-08-13	7.78 (03/14)	No treatment	4 + 3	Unfavorable intermediate risk	13.5	1298.3
MB484-10-14	8.5 (10/14)	No treatment	4 + 3	Unfavorable intermediate risk	12.0	907.9
MB0294PR	4.7 (08/12)	No treatment	4 + 5	High risk	N/A	N/A
MB0496PR	20.63 (11/14)	No treatment	4 + 4	High risk	N/A	N/A
MB0537PR	2.57 (04/15)	No treatment	4 + 4	High risk	N/A	N/A

5. TeloView enabled 3D image analyses and statistical considerations

The TeloView program (3D Signatures Inc., Winnipeg, MB, Canada) is used in this study to analyze the nuclear volume of the CTCs. In this study, it was used to measure the nuclear volumes of each CTC [12–14]. These nuclear volumes are subsequently used to calculate the size of the CTCs (Table).

6. Results

6.1. Prostate CTC nuclear size

Prostate cancer displays different subpopulations of cancer cells present in the same patient [3]. The average size of isolated PCa CTCs may depend on the size of the predominant subpopulation of CTCs isolated at the time point when the blood sample was obtained.

After 3D image acquisition of the isolated PCa CTCs, Teloview software is used to measure the average nuclear volume and nuclear diameter using 30 CTCs from each sample. The 3D imaging of the isolated cells on the filter membrane after staining of their nuclear DNA with DAPI revealed CTC average nuclear diameter greater than the average lymphocyte diameter of 7.3 μm [12]. The Table shows the average nuclear volume and average nuclear diameter (AND) of CTCs isolated from patients with PCa. The average nuclear volume range is from 392 to 1969 μm^3 whereas the AND range is from 9.1 to 15.6 μm. The nuclear sizes are quite variable and suggest that CTC PCa nuclear size does not correlate with risk classification. However, a box-and-whisker plot to study change in CTC size after surgery in comparison with the before surgery reveals no significant change in size (Supplementary Fig. 1).

It has been well established that tumor cells have a high nuclear/cytoplasmic ratio [13]. This fact was confirmed in the isolated PCa CTCs after 3D imaging and analysis.

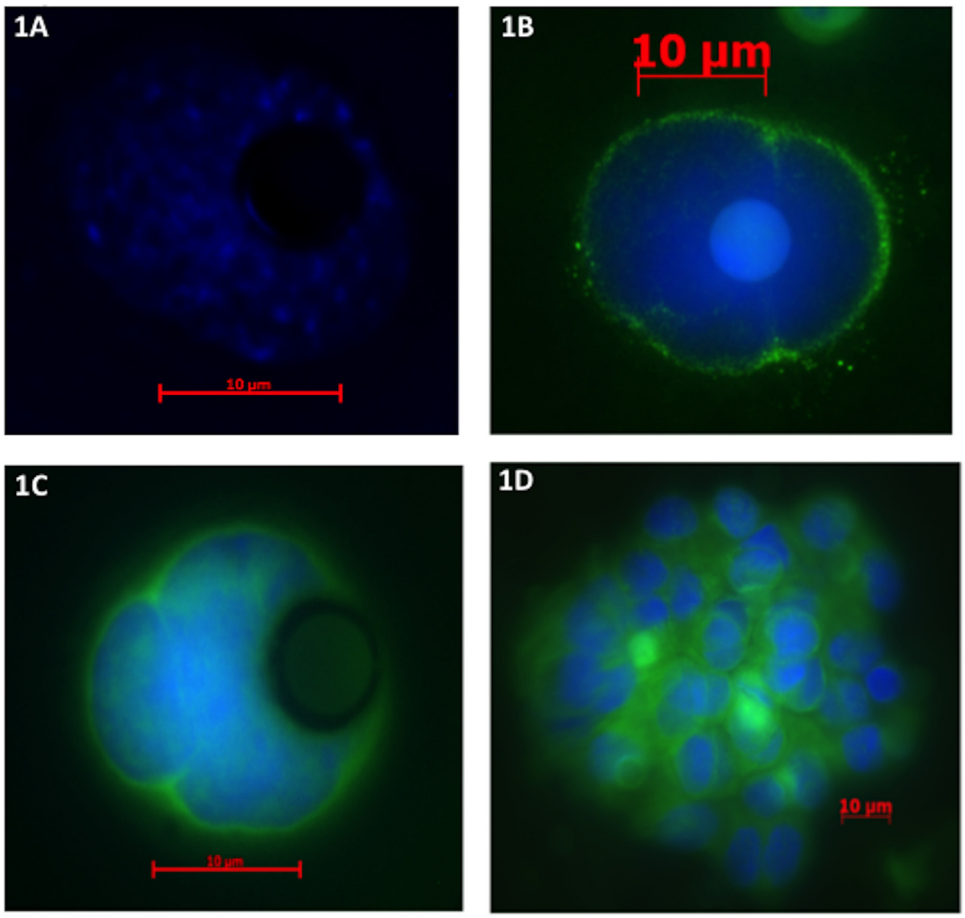

Fig. 1. (A) Nucleus of captured CTC from a patients with low-risk disease MB0322on a filter pore. (B) Cytokeratin (green) stained CTC from MB0339PR, patients with an intermediate-risk disease sample. Nuclear DNA is counterstained with DAPI (blue) with the shadow of a filter pore in the center of the cell. (C) Androgen receptor (AR) stained CTC in patient with low-risk disease (MB0221PR). The cell membrane is distinctly stained green with blue DAPI counterstain of the nuclear DNA. The CTC sits on a filter pore, its out of focus shadow seen on the right of the cell. (D) A CTC cluster stained fluorescent green with Alexa-488 labeled cytokeratin antibody. The presence of CTC clusters has been identified in patients with poor prognosis [23]. (Color version of figure is available online.)

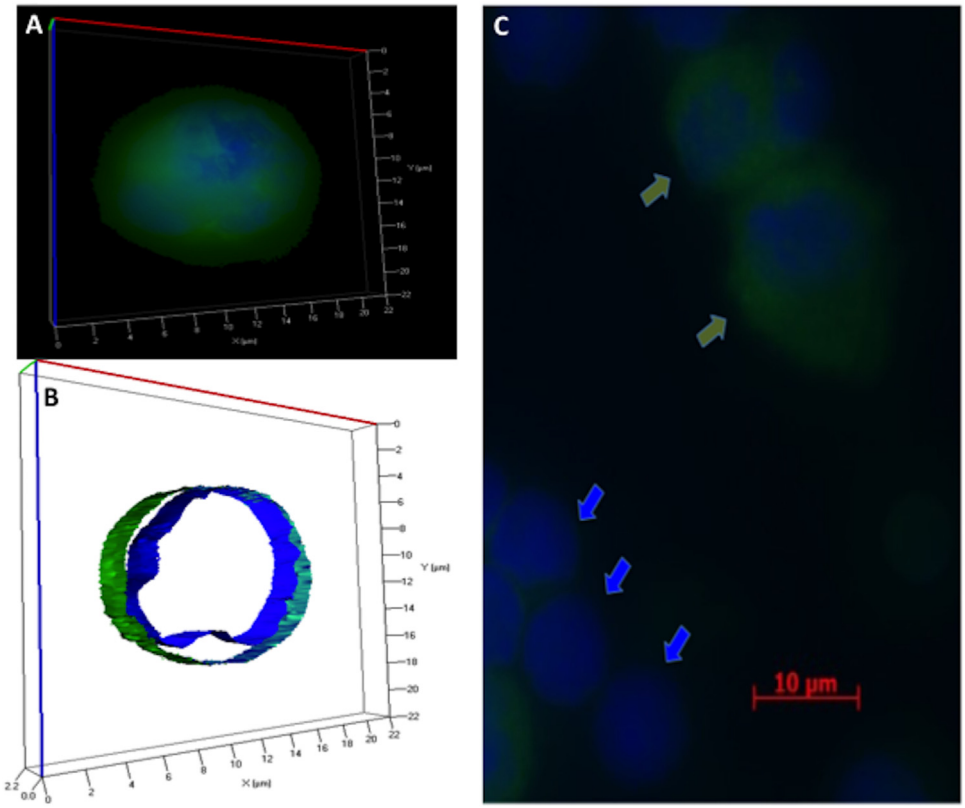

Fig. 2. The isolated CTCs, like other cancer cells have high nuclear/cytoplasmic ratio. (A) 2D and (B) 3D were acquired after the same CTC was cytokeratin stained and the nuclear DNA counterstained with DAPI. A narrow cytoplasmic space is seen on image B, this is a known feature of cancer cells. (C) DAPI stained, but unstained by Alexa 488 tagged secondary antibody to cytokeratin antibody, filter-captured lymphocytes (blue arrows) lying beside 2 PCa CTCs stained green by Alexa 488 tagged secondary antibody to cytokeratin antibody (green arrows). (Color version of figure is available online.)

Fig. 2A and B shows a 3D cross-sectional image of a PCa CTC with a cytokeratin stained CTC membrane and DAPI counterstained nuclear DNA. The CTC membrane diameter measures approximately 14 µm in diameter and the nucleus is approximately 12 µm in diameter. The high nuclear/cytoplasmic ratio can be easily appreciated, as there is only 2 µm of cytoplasm (Fig. 2A and B).

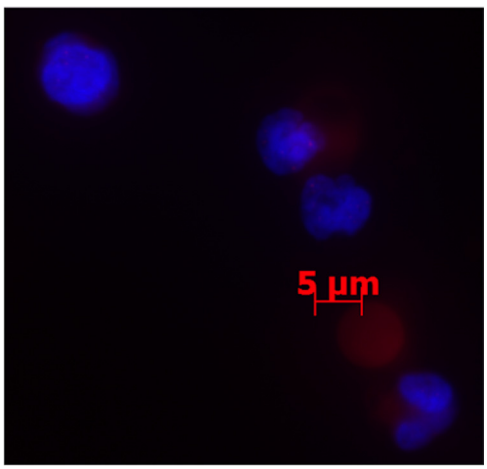

Fig. 3. Female blood passed through the ScreenCell filter captures some lymphocytes that stains negative to androgen receptors. (Color version of figure is available online.)

The smallest AND of PCa CTCs measured in the study is 9.4 µm (Table). The size of the PCa CTCs makes it easy for the CTCs to be captured and prevents them from being filtered through the pores of the ScreenCell filter.

This conclusion is valid for low-risk patients (i.e., MB239) with an average nuclear diameter of 10.8 µm and 11.81 µm comparable with favorable intermediate-risk patients (i.e., MB228) with 10.7 µm average nuclear diameter (Table). The average nuclear diameters of the samples analyzed generally do not correspond with PCa risk stratification (Table). However, blood samples from female controls were passed through the filter device with no PCa CTC found (Fig. 3).

Flow throughs from blood samples passed postfiltration contain debris from red blood cell lysis, lymphocytes, and some CTCs small enough to pass through the filter pores.

6.2. Immunohistochemistry identifies cytokeratin and androgen-positive CTCs in all risk group patients with PCa

CTCs were isolated from all risk group patients by the morphology-based filtration technique used in this study that is highly sensitive and allows for the isolation of PCa CTCs in patients with low- and intermediate-risk disease

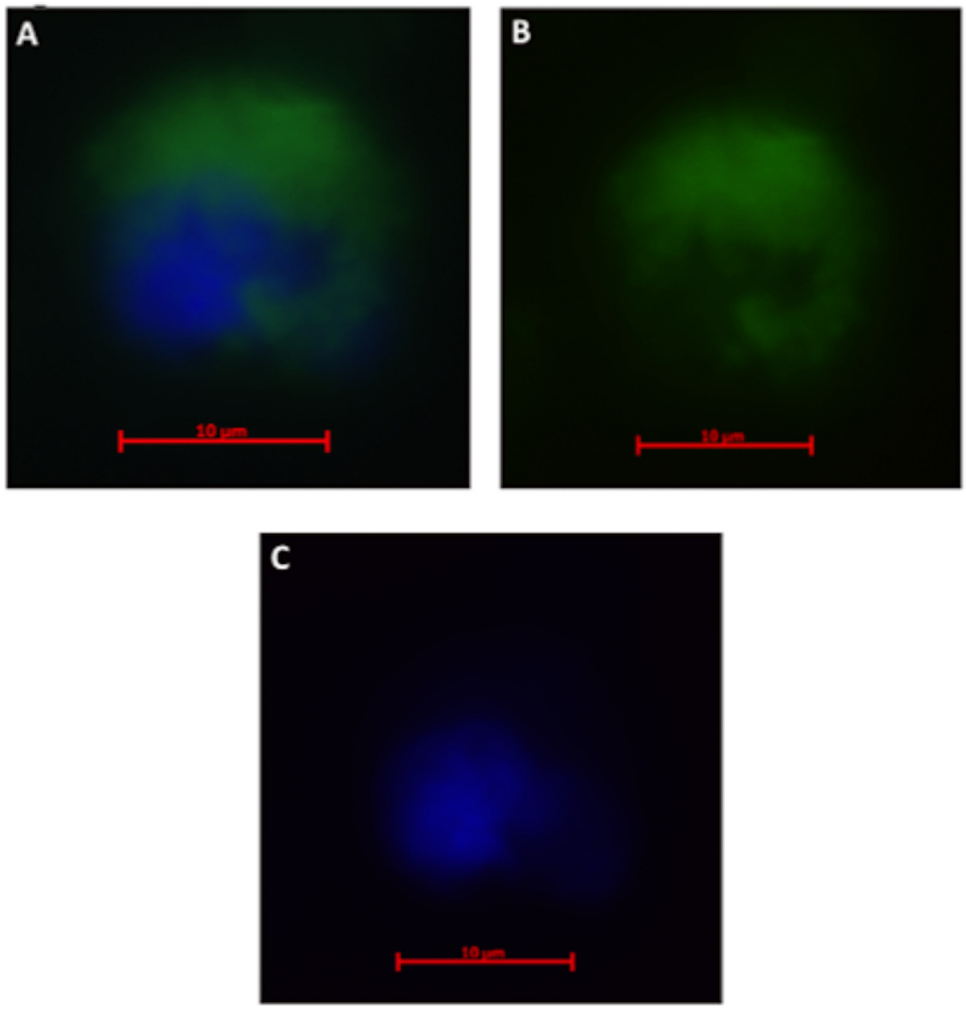

Fig. 4. A CTC from patient with high-risk disease MB0496PR is stained with androgen receptors (AR). AR stains (blue) and DAPI for nuclei DNA (blue) are shown in (A) with the AR prominent in the cytoplasm; AR only in (B); and DAPI only in (C). (Color version of figure is available online.)

[4,14]. In addition, some lymphocytes are captured that fall in between the randomly distributed 10^5 pores on the 8 mm diameter filter and serve as internal, patient-specific controls [4] (Fig. 2).

6.3. Cytokeratin 8, 18, and 19 staining

PCa is an epithelial tumor, the CTCs that are dispersed into the blood stream from primary and secondary sites of PCa express cytokeratins. The isolated CTCs were, therefore, stained for cytokeratins 8, 18, and 19 (Fig. 1B). CTCs from all-risk patient groups stained positive for cytokeratin 8, 18, and 19. The positive immunohistochemical staining of the isolated CTCs of patients with low-, intermediate-, and high-risk disease confirms their epithelial origin. The 2D image acquisitions of the filters display the nuclei of the captured cells in blue and positive cytokeratin immunostained is depicted in green (Fig. 1B). Fig. 2C shows a single PCa CTC (sits on a circular filter pore) stained green with antibodies to cytokeratin 8, 18, and 19 on the cell membrane. Unstained lymphocytes serve as internal controls (Fig. 2). As shown in Fig. 1B, the cytokeratin stain is mainly on the cell membrane surrounding the nucleus. One of the advantages of ScreenCell filtration is the preservation of morphology and clusters of CTCs, and these structures are appreciated observed after immunohistochemistry (Fig. 1D). The nuclear DNA of the cells is shown as DAPI stain (blue) in the images. The staining of CTCs with cytokeratin was not uniform owing to the epithelial mesenchymal transformation. Some PCa CTCs stained in just patches, whereas others stained more uniformly after immunohistochemistry.

6.4. Androgen receptor

The expression of AR by isolated PCa CTCs was assessed by immunohistochemistry. Fig. 1C show CTC isolated from a patient with low-risk disease MB0221PR stained with AR antibody conjugated with Alexa Fluor 488. This further confirms the presence of CTCs in early PCa stages. Unlike cytokeratin stain shown earlier that is mainly a membrane stain, AR stains both the intracytoplasmic

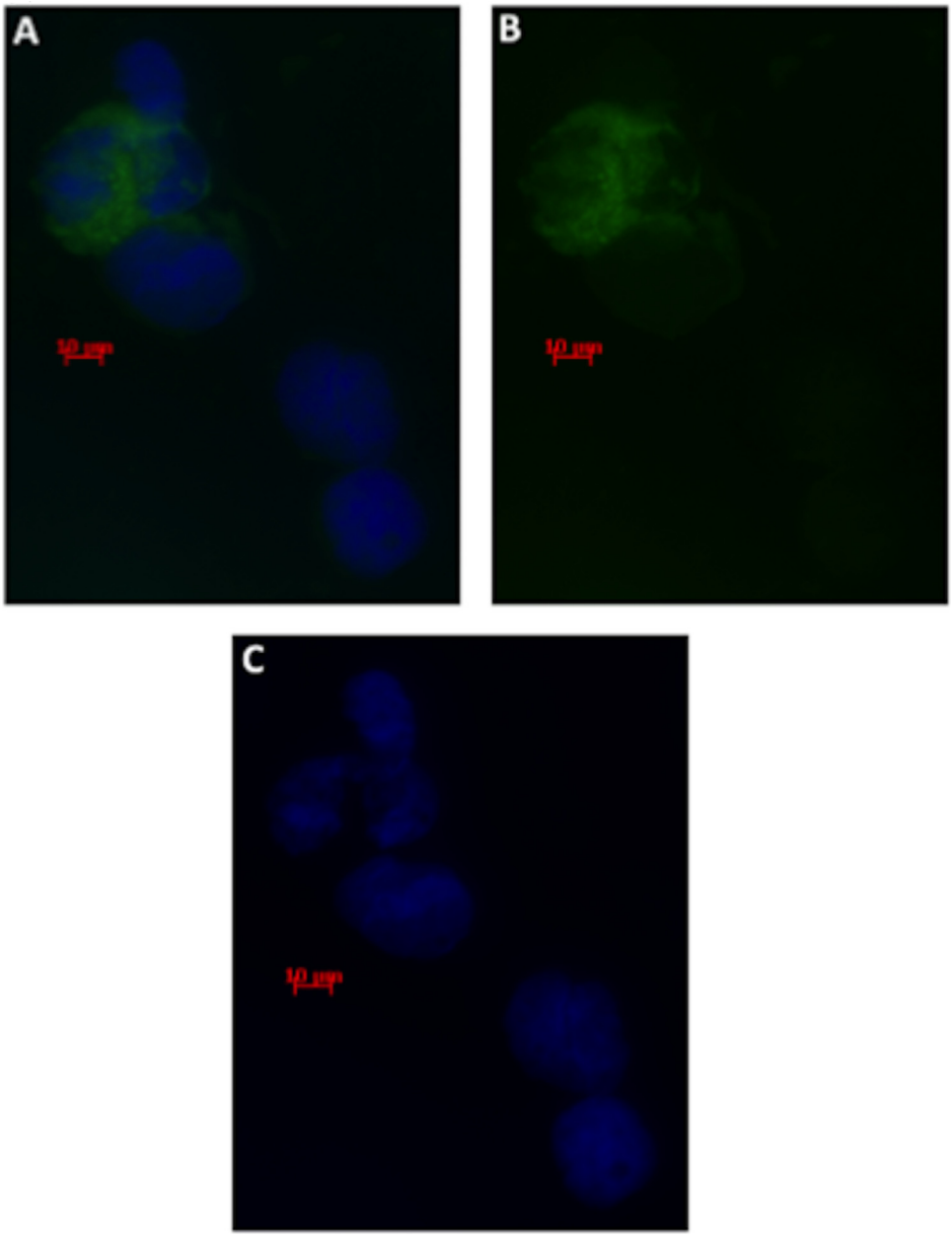

Fig. 5. (A) Positive AR stains (green) on 2 PCa CTCs and positive DAPI stains on the nuclei DNA of the 5 cells: 4 CTCs and 1 lymphocyte (top-most cell). (B) Only the AR (green) stains with the DAPI turned off. (C) Just the DAPI stains on all 5 cells. (Color version of figure is available online.)

region and the cell membrane. Fig. 4 shows CTC from patient with high-risk disease MB0496PR, an example of nuclear DNA engulfed by AR stains in the cytoplasm of CTC (Figs. 1C, 2, 4, and 5).

CTCs from all stages of PCa were stained for AR, the expression of AR on the isolated CTCs was found to be heterogeneous. Figure 5 shows 4 morphologically identified PCa CTCs from patients with high-risk disease MB0294 with average diameter of 30 μm and a lymphocyte (pointed out by red arrow). Two of the CTCs were stained for AR, whereas the other 2 CTCs, and the lymphocytes have negative stain for AR. This finding corresponds with the hypothesis of heterogeneous AR expression PCa as the cancer stage increase [15].

6.5. Combined CD45 and AR staining

CD45 antigen is expressed in all hematopoietic cells except mature red blood cells. Combined AR and CD45 staining was done to identify captured PCa CTCs among hematopoietic cells (Fig. 6) in flow-through cells after filtration. The cells in the flow through are mainly leukocytes that consist of the neutrophils with multilobulated nuclei and lymphocytes both of which stain positive for

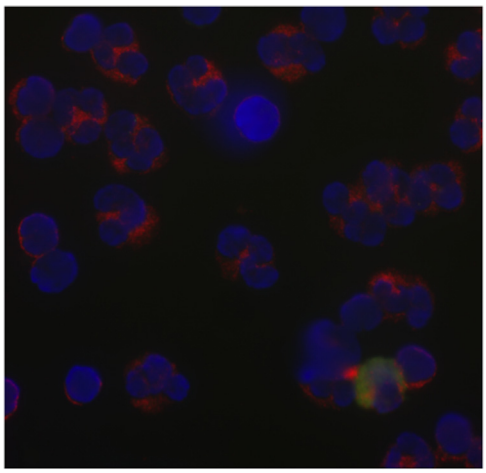

Fig. 6. Flow-though from filtration were centrifuged and mounted on slides. Cell obtained consists of mainly leukocytes, which stain positive to CD45 and a CTC small enough to squeeze through the filter pores that stains positive to AR. (Color version of figure is available online.)

CD45 antigen and negative for AR. Fig. 6 shows a $CD45^{-}$ AR^{+} CTC surrounded by $CD45^{+}AR^{-}$ leukocytes. This depicts an example of CTCs smaller than average size of CTCs being able to go through the pores of the filter.

Fig. 7 shows the staining of a captured CTC on a filter with pores around it, FITC labeled (green) AR labeled stained positive (Fig. 7A), whereas Cy3 labeled CD45 stained negative on the captured PCa CTC.

7. Discussion

The combination of filter-based CTC isolation technique with immunohistochemical staining and 3D imaging followed by analysis of nuclear architecture has indeed presented an opportunity to characterize PCa CTCs in all stages of tumor aggression. This suggests the presence of CTCs is not pathognomonic of advanced or metastatic cancer with poor prognosis and that CTCs can be identified in early-disease states that often have excellent prognosis [16–19]. Our findings support and expand on previous findings in the field. For example, using a microfluidic device, Stott et al. (2010) had described the isolation of CTCs in 16 patients with PCa with localized disease

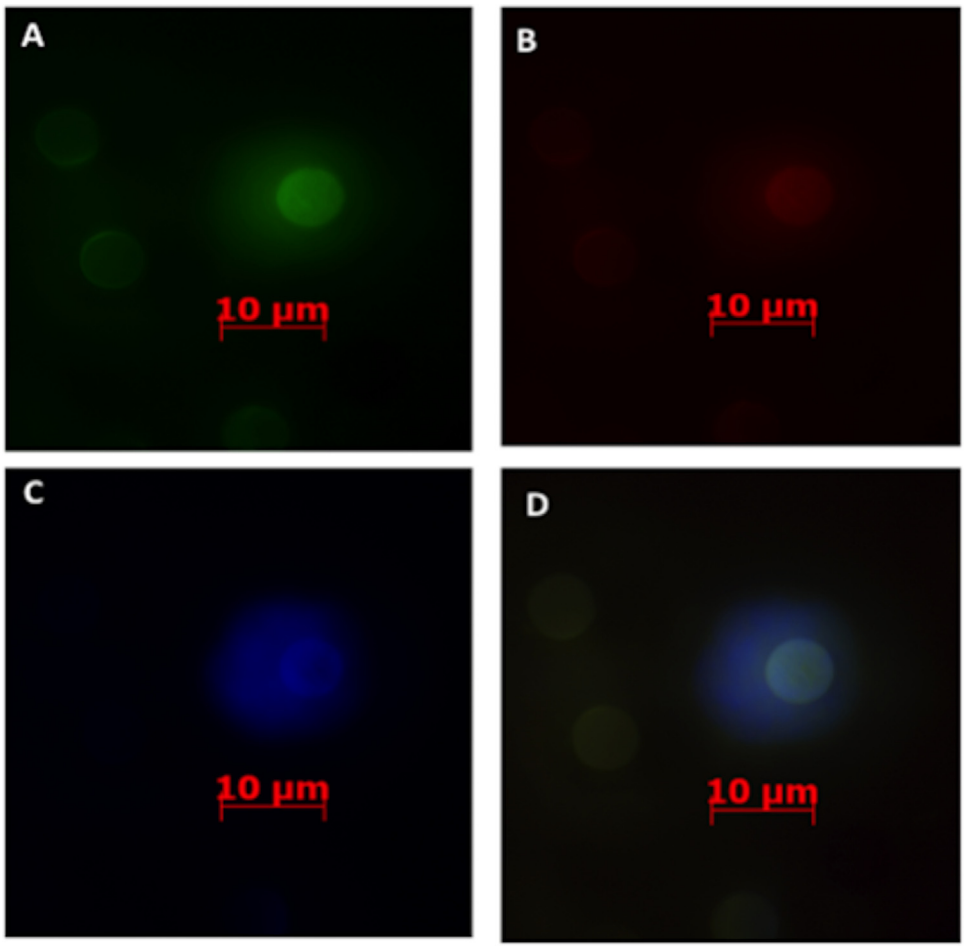

Fig. 7. Combined AR and CD45 staining of isolated CTC on a filter stains positive for AR and negative for CD45. (Color version of figure is available online.)

(Gleason score 6 and 7) as well as in 4 patients with high-risk disease (Gleason score 8 and 9) before any medical intervention and after surgery. In a similar manner, Kolostova et al. (2014) found CTCs in localized PCa using MetaCell, a filtration device different from that used in our study (pore size: 8 μm). The authors reported that 52% of the enrolled patients with localized disease exhibited CTCs. The discrepancy of these numbers with the ones reported by Stott et al. (2010) and in our study is unknown, but may be dependent on the patient cohort or the pore sizes or both of MetaCell and the microfluidics tool used by Stott et al. However, Lin (2010) made use of a model microdevice filter and obtained a recovery rate of 92%, which is similar to the ScreenCell filter recovery rate [20].

CTCs dispersed into blood circulation from primary and secondary PCa sites undergo epithelial to mesenchymal transition [21]. This transition can cause down-regulation of antibodies such as EPCAM that are expressed in epithelial tumors. Low-EPCAM or non-EPCAM are not captured by antibody dependent enrichment methods and may result in an incomplete analysis. Most, if not all of these CTC subpopulation groups are captured with the ScreenCell filter. A potential drawback to a size-based filtration techniques is "over collection" owing to other blood cells that may remain on the filter. Debris from lyzed red blood cells fall through the filter pores. The filters, sometimes, capture lymphocytes when they fall between pores, the average size of lymphocytes have been estimated to 7.02 μm, range: 5.81 to 8.14 μm measured by colter counter and 6.05 μm measured by flow cytometer, range: 4.92 to 7.25 μm, both measurements of 11,000 to 70,000 cells from 3 donors [12]. The captured lymphocytes are easily differentiated from PCa CTCs, because the nuclei of the lymphocytes are dense and are approximately the size of the filter pores (7.5 μm) unlike CTC nuclei, which are larger (9.1–15.6 μm) [22]. Moreover, the lymphocytes are CD45+, whereas the CTCs captured did not show this marker.

This article gives insights into the opportunity to further characterize CTCs of patients with PCa at the early (and later) stages of cancer development in a sequential manner without the need for multiple biopsies. Owing to the nature of CTCs being "liquid biopsies", they can be obtained more frequently and represent the tumor tissue more precisely than prostate core biopsies.

8. Conclusion

The isolation of CTCs from patients with PCa independent of risk groups and stages or forms of management of PCa provides a viable platform for the study of CTCs in PCa. We have shown that analysis and characterization of PCa CTCs in all risk groups can be achieved with CTCs captured on filters.

Author contribution

S.M., D.D., J.S., and J.A.A. designed the experiments, analyzed the data and edited the article. J.A.A. isolated the PCa CTCs, performed immunohistochemistry, and imaged the CTCs.

Competing interest

S.M. is a cofounder, director, and chair of the Clinical and Scientific Research Advisory Board of 3D Signatures Inc.

Acknowledgment

We thank the patients for their participation in this study and 3D Signatures Inc. for the use of TeloView. We thank Dr. Naoual Benali-Furet for an aliquot of anti-CD45 antibody. The Manitoba Motorcycle Ride For Dad (SM), Movember GAP1 CTC (SM), and a MITACS Accelerate fellowship to J.A.A. supported this study.

Appendix A. Supporting information

Supplementary data associated with this article can be found in the online version at http://dx.doi.org/10.1016/j.urolonc.2016.12.008.

References

[1] Ashworth TR. A case of cancer in which cells similar to those in the tumors were seen in the blood after death. Aust Med J 1869;14:146–9.
[2] Miller MC, Doyle GV, Terstappen LW. Significance of circulating tumor cells detected by the cellsearch system in patients with metastatic breast colorectal and prostate cancer. J Oncol 2010;2010:617421.
[3] Adebayo Awe J, Xu MC, Wechsler J, Benali-Furet N, Cayre YE, Saranchuk J, et al. Three-dimensional telomeric analysis of isolated circulating tumor cells (CTCs) defines CTC subpopulations. Transl Oncol 2013;6:51–65.
[4] Desitter I, Guerrouahen BS, Benali-Furet N, Wechsler J, Janne PA, Kuang Y, et al. A new device for rapid isolation by size and characterization of rare circulating tumor cells. Anticancer Res 2011;31:427–41.
[5] de Bono JS, Scher HI, Montgomery RB, Parker C, Miller MC, Tissing H, et al. Circulating tumor cells predict survival benefit from treatment in metastatic castration-resistant prostate cancer. Clin Cancer Res 2008;14:6302–9.
[6] Cohen SJ, Punt CJ, Iannotti N, Saidman BH, Sabbath KD, Gabrail NY, et al. Relationship of circulating tumor cells to tumor response, progression-free survival, and overall survival in patients with metastatic colorectal cancer. J Clin Oncol 2008;26:3213–21.
[7] Kongruttanachok N, Cayre YE, Knecht H, Mai S. Rapid separation of mononuclear hodgkin from multinuclear reed-sternberg cells. Lab Hematol 2014;20:2–6.
[8] Iwanicki-Caron I, Basile P, Toure E, Antonietti M, Lecleire S, Di Fiore A, et al. Usefulness of circulating tumor cell detection in pancreatic adenocarcinoma diagnosis. Am J Gastroenterol 2013;108:152–5.

[9] Chen CL, Mahalingam D, Osmulski P, Jadhav RR, Wang CM, Leach RJ, et al. Single-cell analysis of circulating tumor cells identifies cumulative expression patterns of EMT-related genes in metastatic prostate cancer. Prostate 2013;73:813–26.
[10] Society CC: Canadian Cancer Society's Advisory Committee on Cancer Statistics. Inc.; 2015.
[11] D'Amico AV, Whittington R, Schultz D, Malkowicz SB, Tomaszewski JE, Wein A. Outcome based staging for clinically localized adenocarcinoma of the prostate. J Urol 1997;158:1422–6.
[12] Kuse R, Schuster S, Schubbe H, Dix S, Hausmann K. Blood lymphocyte volumes and diameters in patients with chronic lymphocytic leukemia and normal controls. Blut 1985;50:243–8.
[13] Incze J, Vaughan CW Jr., Lui P, Strong MS, Kulapaditharom B. Premalignant changes in normal appearing epithelium in patients with squamous cell carcinoma of the upper aerodigestive tract. Am J Surg 1982;144:401–5.
[14] Vona G, Sabile A, Louha M, Sitruk V, Romana S, Schutze K, et al. Isolation by size of epithelial tumor cells: a new method for the immunomorphological and molecular characterization of circulating-tumor cells. Am J Pathol 2000;156:57–63.
[15] Punnoose EA, Ferraldeschi R, Szafer-Glusman E, Tucker EK, Mohan S, Flohr P, et al. PTEN loss in circulating tumour cells correlates with PTEN loss in fresh tumour tissue from castration-resistant prostate cancer patients. Br J Cancer 2015;113:1225–33.
[16] Nakagawa T, Martinez SR, Goto Y, Koyanagi K, Kitago M, Shingai T, et al. Detection of circulating tumor cells in early-stage breast cancer metastasis to axillary lymph nodes. Clin Cancer Res 2007;13:4105–10.
[17] Rahbari NN, Aigner M, Thorlund K, Mollberg N, Motschall E, Jensen K, et al. Meta-analysis shows that detection of circulating tumor cells indicates poor prognosis in patients with colorectal cancer. Gastroenterology 2010;138:1714–26.
[18] Bobek V, Gurlich R, Eliasova P, Kolostova K. Circulating tumor cells in pancreatic cancer patients: enrichment and cultivation. World J Gastroenterol 2014;20:17163–70.
[19] Alsaadi H, Awe JA, Wark L, Bassi J, Saranchuk J, Drachenberg D, et al. Enumeration and morphological features of CTCs in all risk groups of localized and metastatic prostate cancer using size-based filtration. Under revision 2016.
[20] Lin HK, Zheng S, Williams AJ, Balic M, Groshen S, Scher HI, et al. Portable filter-based microdevice for detection and characterization of circulating tumor cells. Clin Cancer Res 2010;16:5011–8.
[21] Zhu ML, Kyprianou N. Role of androgens and the androgen receptor in epithelial-mesenchymal transition and invasion of prostate cancer cells. FASEB J 2010;24(3):769–77.
[22] Wood EJ. Cellular and molecular immunology. Abbas AK, Lichtman AH, 5th ed. Biochemistry and Molecular Biology Education, 5th ed., 32; 2004;65–6.
[23] Aceto N, Bardia A, Miyamoto David T, Donaldson Maria C, Wittner Ben S, Spencer Joel A, et al. Circulating Tumor cell clusters are oligoclonal precursors of breast cancer metastasis. Cell 2014;158(5):1110–22.